Lagrangian Q-criterion and Transport of Salt and Temperature

S. Wolligandt J. Zimmermann T. Wilde M. Motejat H. Theisel

ABSTRACT

We analyze the IEEE SciVis contest 2020 data set. To detect eddies in the *Red Sea*, we use a Lagrangian Q criterion. Based on this, we confirm two eddies in the *Red Sea* that are consistent on the first three ensemble members, and only one eddy consistent over the first six ensemble members.

To analyze the transport of salt and temperature, we propose a two-step visualization. First, we color code temperature/salinity as 2D time-dependent scalar fields. Second, we integrate particles with color coding the change of temperature/salinity along their paths. Based on this we can distinguish regions dominated by transport from regions where other effects are relevant.

1 Introduction and Notation

Fluid flows can be represented as N-dimensional vector fields, where mostly $N = 2$ or $N = 3$. At each position $\mathbf{x} \in D$ of a spatial domain $D \subset \mathbb{R}^N$ and at each time $t \in T$ of a temporal domain $T \subset \mathbb{R}$ a vector $\mathbf{v}(\mathbf{x},t) \in \mathbb{R}^N$ is defined. The jacobian of a vector field $\mathbf{v}$ will be denoted as $\mathbf{J}$, where $\mathbf{J}(\mathbf{x},t) = \nabla\mathbf{v}(\mathbf{x},t)$. Another important property of flows are its integral curves, also knows as path lines. Path lines are denoted as $\mathscr{P}$ and are defined as follows:

$$\begin{aligned} \frac{\partial \mathscr{P}(\mathbf{x}_0,t_0,\tau)}{\partial \tau} &= \mathbf{v}(\mathscr{P}(\mathbf{x}_0,t_0,\tau),t_0+\tau) \\ \mathscr{P}(\mathbf{x}_0,t_0,0) &= \mathbf{x}_0 \end{aligned} \tag{1}$$

In this paper the 3-dimensional water flow of the *Red Sea* will be denoted as $\mathbf{v}(\mathbf{x},t)$ where D is the area inside the bathymetry of the *Red Sea* and part of the *Gulf of Aden* and T is in the range of 0 to 30 days. Additionally, salinity and temperature are given. Both of these properties can be represented as time-dependent scalar fields $\mathscr{S}(\mathbf{x},t)$ [salinity] and $\mathscr{T}(\mathbf{x},t)$ [temperature]. The data is given as an ensemble data set. An ensemble member is denoted with the index $i \in [1..50]$ (e.g. $\mathbf{v}_1(\mathbf{x},t)$). Each ensemble member $\mathbf{v}_i$ of the whole ensemble share D and T. Due to perturbations of the initial conditions of the simulations different flow behaviors take place at the same position for two different ensemble members $\mathbf{v}_i$ and $\mathbf{v}_j$.

2 Lagrangian Q-criterion to detect Eddies

"Eddies are clockwise or counter-clockwise circular movements of water that play a major role in transporting energy and biogeochemical particles in the ocean" (from [1]). Eddies are related but not identical to vortices. Similar to vortices, there are various competing definitions of eddies. We chose an eddy concept of a Lagrangian Q-criterion. The Q-criterion is a standard local Galilean invariant vortex criterion. Since eddies are related to water transport, we observe Q not only locally but in a Lagrangian way: we measure and visualize the time that a particle stays within a Q-zone during integration. Details follow below.

Lagrangian View Flows can be observed in different ways [9]. One way is the eulerian view. Here a property of a flow $\mathbf{v}$ is observed at a stationary position $\mathbf{x}$ with varying time t.

Another way is the Lagrangian view. In this view the observer position changes over time via advection of the flow. This means that $\mathbf{x}$ moves along a path line $\mathscr{P}(\mathbf{x}_0,t_0,\tau)$ of a flow $\mathbf{v}$ that originates at $\mathbf{x}_0$, t_0 with increasing or decreasing time τ. This way one captures not only the properties of one single point of the flow but also the flow itself. That is the reason why a Lagrangian view is better suited to detect eddies.

Eddy detection techniques There are two big classes of how eddies can be detected: region-based and line-based. The latter tries to extract the centers of eddies as a curve. (e.g. Sujudi and Haimes [11] and the *Parallel Vectors Operator* by Peikert and Roth [8]).

Example methods for region-based detection of eddies are e.g. the λ_2 [5], vorticity magnitude [7], [10] and the *Q-criterion* [4]. For an overview of eddy / vortex detection see [2].

For our detection method we focus on region-based detection and more specifically the *Q-criterion*.

Our eddy detection technique However, this definition of an eddy leads to regions where *one* stationary position in the domain of the flow has rotating behavior. The more interesting question is if a *particle* stays in a region where the Q-criterion is fulfilled for a certain time. This check can be done by measuring Q at the position of a particle as it is advected by the flow which corresponds to the Lagrangian view.

Haller [3] introduced this concept with his hyperbolic trajectories (HTs) not using the property Q but the hyperbolicity h. A HT is defined as the trajectory of massless particles that is advected by $\mathbf{v}$ namely a path line $\mathscr{P}$ where each point $\mathbf{x} \in \mathscr{P}$ is in a hyperbolic region ($h(\mathbf{x},t) > 0$). That means a hyperbolic trajectory has *maximum-hyperbolicity-time*. For the sake of detecting eddies we replace the property h by Qb (see equation 2) so that we get maximum-Q-time.

$$Qb(\mathbf{x},t) = \begin{cases} 1 & \text{if } Q(\mathbf{x},t) > 0 \\ 0, & \text{otherwise} \end{cases} \tag{2}$$

We relax the condition of maximum-Q-time. Instead of having a binary observation (maximum- or non-maximum-Q-time) we measure the physical time of how long a particle stays in a region where $Q > 0$ which we call the *Q-time* $\mathscr{Q}_\tau \in [0..1]$ (see equation 3). 1 means a particle moves solely in regions where $Q > 0$ (maximum-Q-time). 0 means a particle never moves into a region where $Q > 0$. Additionally, we check if the Q-criterion is fulfilled at the initial position of the path line. If not $\mathscr{Q}_\tau$ becomes 0. This excludes positions where particles start at non-eddy regions and are advected into an eddy region later.

$$\mathscr{Q}(\mathbf{x},t)_\tau = Qb(\mathbf{x},t) \cdot \frac{1}{\tau} \int_t^{t+\tau} Qb(\mathscr{P}(\mathbf{x},t,\tau),t+\tau)\, d\tau \tag{3}$$

The $\mathscr{Q}_\tau$ is a normalized property since we divide by the actual lifetime τ of a particle.

3 Transport of Salt and Temperature

The temporal evolution of temperature/salinity is governed by two physical processes: transport and diffusion. To analyze the transport, we chose the following approach:

- Temperature/salinity are time-dependent scalar fields that are simply color coded over time. Since the flow is dominated by horizontal components, this can be done in 2D.

- In addition, we integrate particles and equip them with a color coding of the change of temperature/salinity. If temperature/salinity were only influenced by transport, particle had a constant temperature/salinity along its life. Any shown changes in temperature/salinity refer to effects different from transport: diffusion, boundary conditions (heating at water surface), and uncertainty.

We use up to 600,000 particles, which are randomly seeded at sea level. The trajectory of every massless particle is described as a path line 1. We track the salinity and temperature on each path line and calculate the change in time 4.

$$\begin{aligned} \text{change of salt along } \mathscr{P} &= \frac{\partial \mathscr{S}(\mathscr{P}(\mathbf{x}_0,t_0,\tau),t_0+\tau)}{\partial \tau} \\ \text{change of temperature along } \mathscr{P} &= \frac{\partial \mathscr{T}(\mathscr{P}(\mathbf{x}_0,t_0,\tau),t_0+\tau)}{\partial \tau} \end{aligned} \tag{4}$$

With a sufficient amount of particles, regions of similar and rapid changing properties can be recognized. We use a diverging colormap with an addition of transparency for near 0 change of $\mathscr{S}$ and $\mathscr{T}$ along the pathlines. As those particles do not provide more insight than the flow behavior itself, it is possible to observe the actual $\mathscr{S}$ and $\mathscr{T}$.

4 Results

4.1 Eddy Detection

In summary, we detected several temporally consistent eddies (between 3 and 10) in each ensemble member (We consider only the *Red Sea* and disregard the eddies in the *Gulf of Aden*). However, an ensemble analysis shows that most of the eddies are not consistent over several ensemble members. In fact, we confirm only two eddies that are consistent over the first three ensemble members and only one eddy consistent over the first six ensemble members.

We compare Q and $\mathscr{Q}$ visually for three ensemble members $\mathbf{v}_{\{1,2,3\}}$ and additionally show the mean of Q and $\mathscr{Q}$ for these three members. The images at figures 1, 2, 3 and 4 are direct volume renderings [6] of Q and $\mathscr{Q}$ and additionally show the bathymetry and the shore line of the *Red Sea* and part of the *Gulf of Aden*. We have chosen an integration length of $\tau = 10$ days ($\mathscr{Q}_{10}$) for the visualizations. $\mathscr{Q}_{10}(\mathbf{x},t) = 1$ means that a particle started at a position $\mathbf{x}$ and time t keeps in the eddy for 10 days, $\mathscr{Q}_{10}(\mathbf{x},t) = 0.5$ for 5 days. Figures 1 and 2 show $\mathscr{Q}_{10}$ and Q side by side.

Figure 1 varies time of $\mathbf{v}_1$: Q is very cluttered and vanishes over time. It seems to "waver" when animated. $\mathscr{Q}_{10}$ shows clearer and more homogeneous "tornado-like" structures that seem to swirl when animated (see the movie for this). The structures of $\mathscr{Q}_{10}$ also vanish with increasing time.

Figure 2 keeps time constant at $t = 100h$ and shows $\mathbf{v}_{\{1,2,3\}}$: As in figure 1 $\mathscr{Q}_{10}$ is less cluttered than Q and has more homogeneous structures. Both $\mathscr{Q}_{10}$ and Q do not seem to correlate for different ensemble members.

However, in the middle row of figures 3 and 4 two regions can be seen where the ensembles in average have eddies for at least 6 days. The bottom rows show the mean of $\mathscr{Q}_{10}$ for $\mathbf{v}_{\{1,2,3,4,5,6\}}$. Here the eddy regions are clearly getting weaker and particles in average only stay for 3 days in eddies. At $t = 200h$ there is only the northern eddy present.

Performance Computing the $\mathscr{Q}$ field takes rather long even when run on a machine with 20 CPU cores at 2.6 GHz and 100 GB RAM. We are doing an adaptive *Runge-Kutta-43* integration at each grid vertex position of the original grid of the dataset and construct a polyline which represents the pathline. Additionally Q has to be computed at each control point of the polyline. For one single ensemble member it took between 1 and 1.5 days for calculating $\mathscr{Q}$ for every second hour of the whole time domain (354 time for one ensemble member).

Because of this we were only able to analyze six out of 50 ensemble members.

4.2 Transport of Salt and Temperature

We compare three consecutive time steps of $\mathbf{v}_1$ and $\mathbf{v}_{mean}$ which have a temporal distance of 15 minutes each, starting from the very first time slice. Figure 5 shows this for the salinity, giving information about regions of particles, which mostly increase the salinity. Ensemble 1 and the mean indicate that salinity increases slightly right after the flow from the *Gulf of Aden* into the *Red Sea*. The greatest region of salinity increase, sits in the center of the *Red Sea*. This is where lower salinity water from the *Gulf of Aden* mixes with high salinity from the upper half of the *Red Sea*. As it can not be observed in the images, there is an eddy at that location, which can be observed in the videos. This gets even clearer in comparison to the mean, as the regions of salinity change are less scattered. Figure 6 shows three time slices, $\mathbf{v}_1$, $\mathbf{v}_2$ and $\mathbf{v}_3$, with a temporal distance of 100 hours each. It can be observed that the change of salinity for particles smooth out with advancing time in all three ensemble members. Another observation is that the different outlines of salinity increase across the ensemble members but with a concentration in the center of the red sea. This can be observed even through the smoother information at 100 and 200 hours. Figure 7 compares $\mathbf{v}_1$ with $\mathbf{v}_{mean}$ with respect to temperature and its change. Just as the salinity, the change of temperature is mostly positive. The regions of up-heat in $\mathbf{v}_{mean}$ are much smaller but remain mostly in the same place as in $\mathbf{v}_1$. The videos are also indicating, that those regions of up-heat are relative stable even if they smooth out over time. This can be observed in figure 8 and the video. In summary, with respect to the additional flow information from the video, it is most likely that certain eddies distribute water with lower salinity from the *Gulf of Aden* into the northern part of the *Red Sea*. Furthermore, the videos show eddies which consist of regions of heating and cooling. For example eddies in the *Gulf of Aden* indicate that water is heating up in certain regions of an eddy while it cools down in another part. This can be interpreted as the mixing of water with different temperatures since the average temperature in an eddy remains the same.

Acknowledgements: This work was partially supported by DFG grants TH 692/14-1 and TH 692/17-1.

References

[1] `https://kaust-vislab.github.io/SciVis2020/`.
[2] T. Günther and H. Theisel. The state of the art in vortex extraction. *Computer Graphics Forum*, 37(6):149–173, 2018.
[3] G. Haller. Finding finite-time invariant manifolds in two-dimensional velocity fields. *Chaos (Woodbury, N.Y.)*, 10:99–108, 04 2000. doi: 10.1063/1.166479
[4] J. Hunt, A. Wray, and P. Moin. Eddies, streams, and convergence zones in turbulent flows. *Studying Turbulence Using Numerical Simulation Databases*, -1:193–208, 11 1988.
[5] J. Jeong and F. Hussain. Hussain, f.: On the identification of a vortex. jfm 285, 69-94. *Journal of Fluid Mechanics*, 285:69 – 94, 02 1995. doi: 10.1017/S0022112095000462
[6] A. Kaufman and K. Mueller. *Overview of Volume Rendering*, vol. 7, pp. 127–XI. 12 2005. doi: 10.1016/B978-012387582-2/50009-5
[7] J. Kim, P. Moin, and R. Moser. The turbulence statistics in fully developed channel flow at low reynolds number. *Journal of Fluid Mechanics*, 177, 05 1987. doi: 10.1017/S0022112087000892
[8] R. Peikert and M. Roth. The "parallel vectors" operator - a vector field visualization primitive. In *IEEE Visualization*, pp. 263–270, 1999.
[9] J. Price. Lagrangian and eulerian representations of fluid flow: Kinematics and the equations of motion. 07 2006.
[10] F. Sadlo, R. Peikert, and E. Parkinson. Vorticity based flow analysis and visualization for pelton turbine design optimization. pp. 179 – 186, 11 2004. doi: 10.1109/VISUAL.2004.128
[11] D. Sujudi and R. Haimes. Identification of swirling flow in 3-d vector fields, 1995.

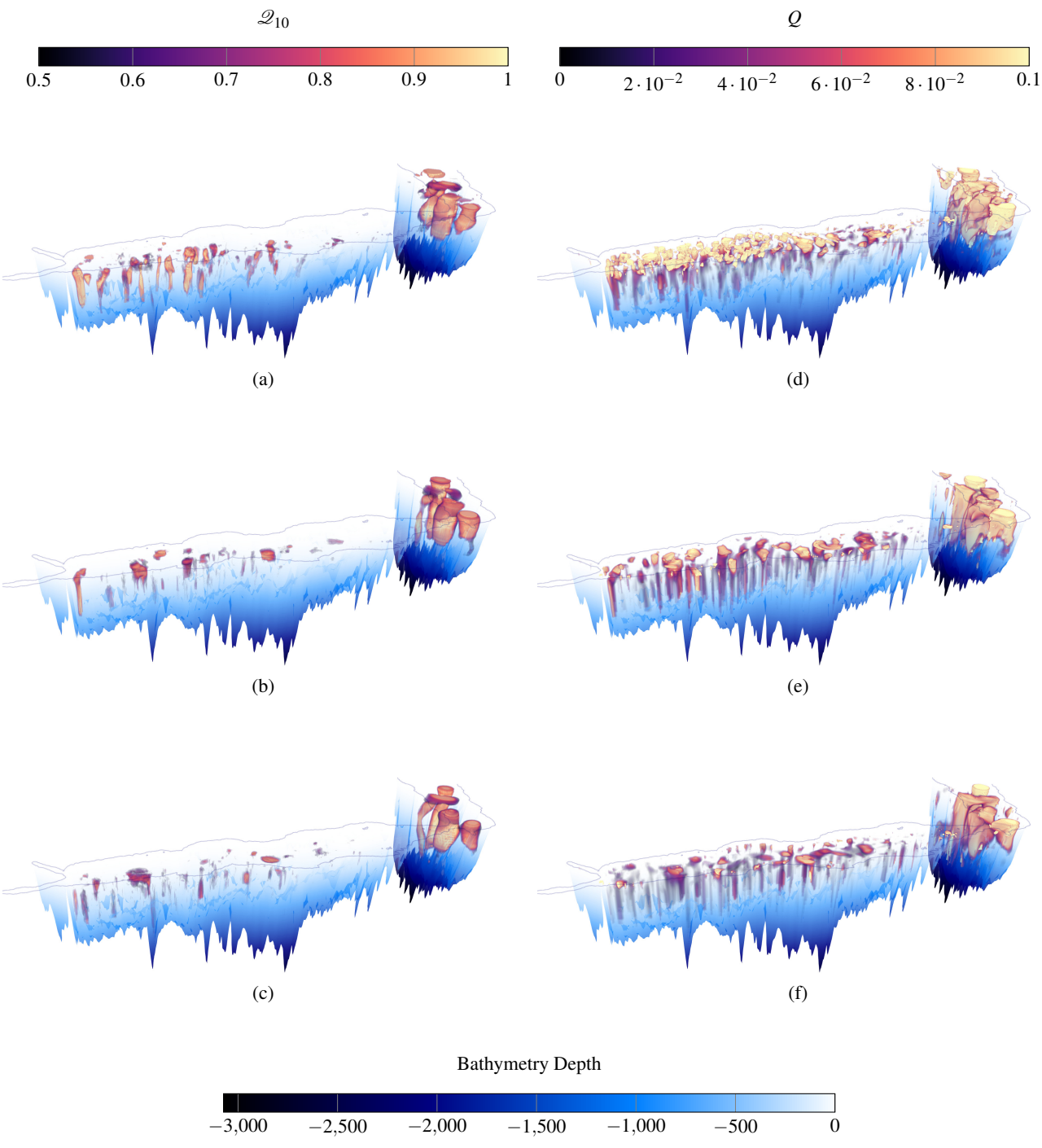

Figure 1: $\mathbf{v}_1$ with varying t. Left: $\mathscr{Q}_{10}$, right Q. Top: $t = 0$h, center: $t = 100$h, bottom: $t = 200$h.

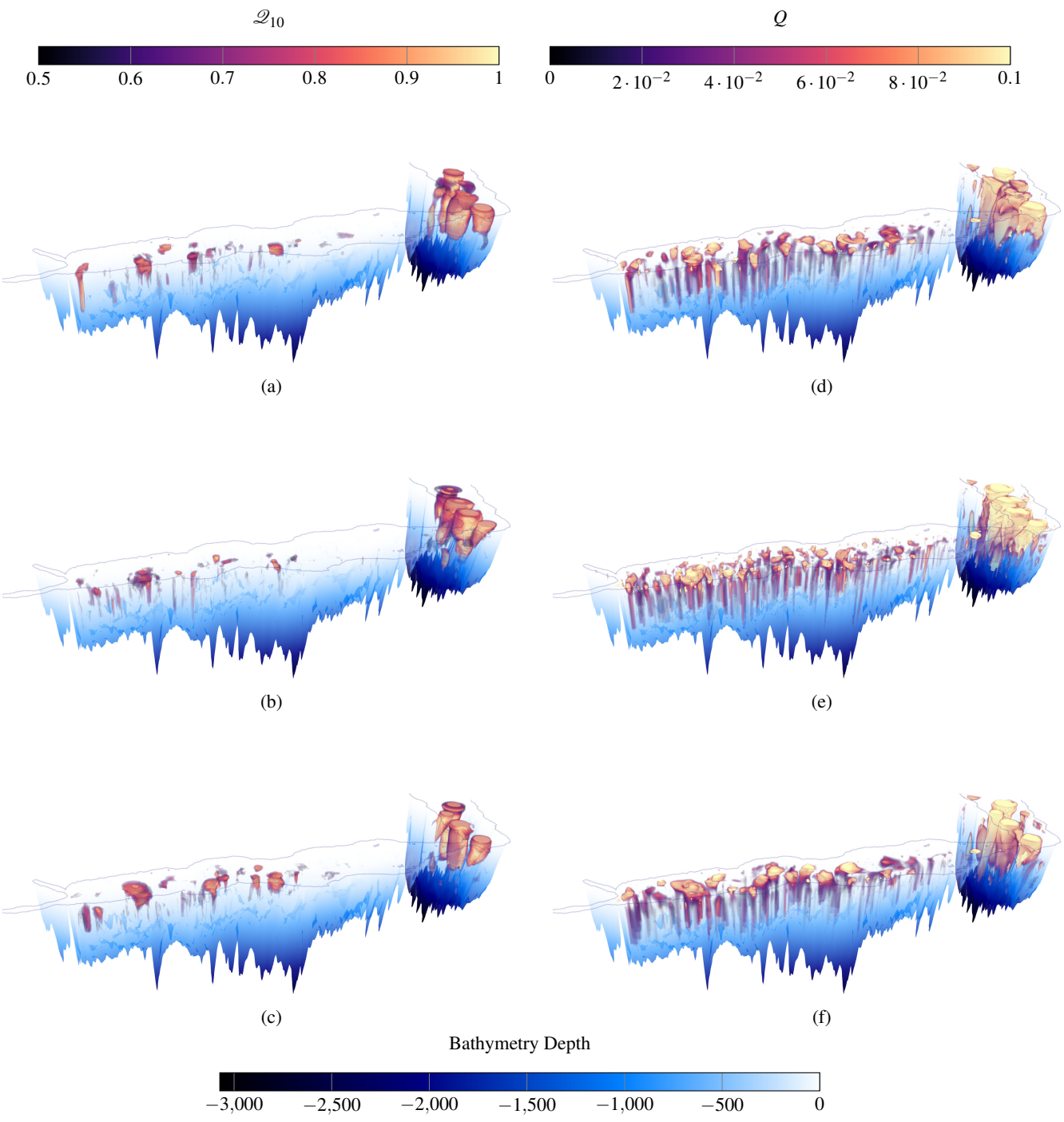

Figure 2: Fixed time at $t = 100$h. Left: $\mathscr{Q}_{10}$, right Q. Top: $\mathbf{v}_1$, center: $\mathbf{v}_2$, bottom: $\mathbf{v}_3$ 3.

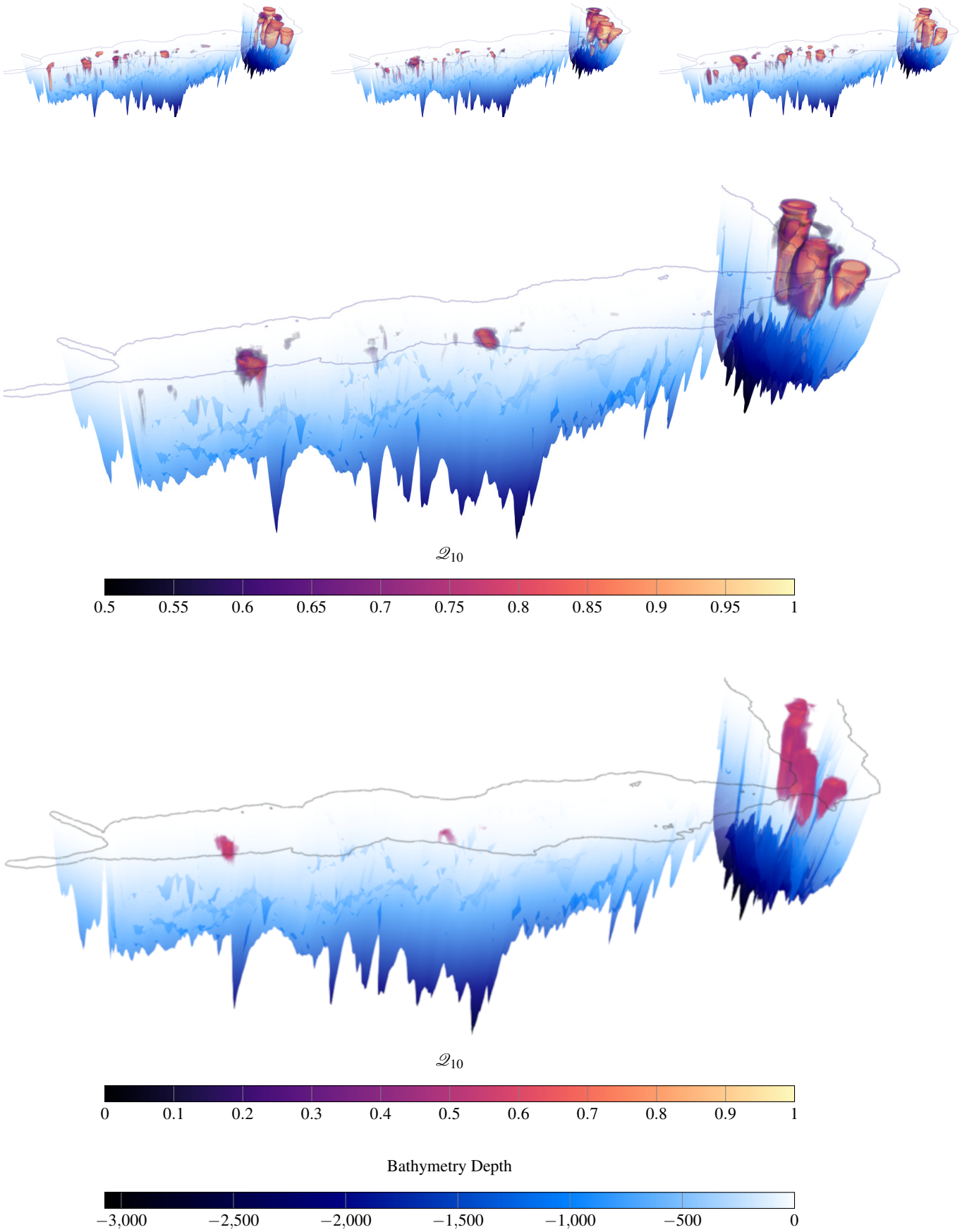

Figure 3: Top: $\mathscr{Q}_{10}$ of $\mathbf{v}_{\{1,2,3\}}$ at time $t = 100$h. Middle: Mean of $\mathscr{Q}_{10}$ for $\mathbf{v}_{\{1,2,3\}}$; Bottom Mean of $\mathscr{Q}_{10}$ for $\mathbf{v}_{\{1,2,3,4,5,6\}}$;

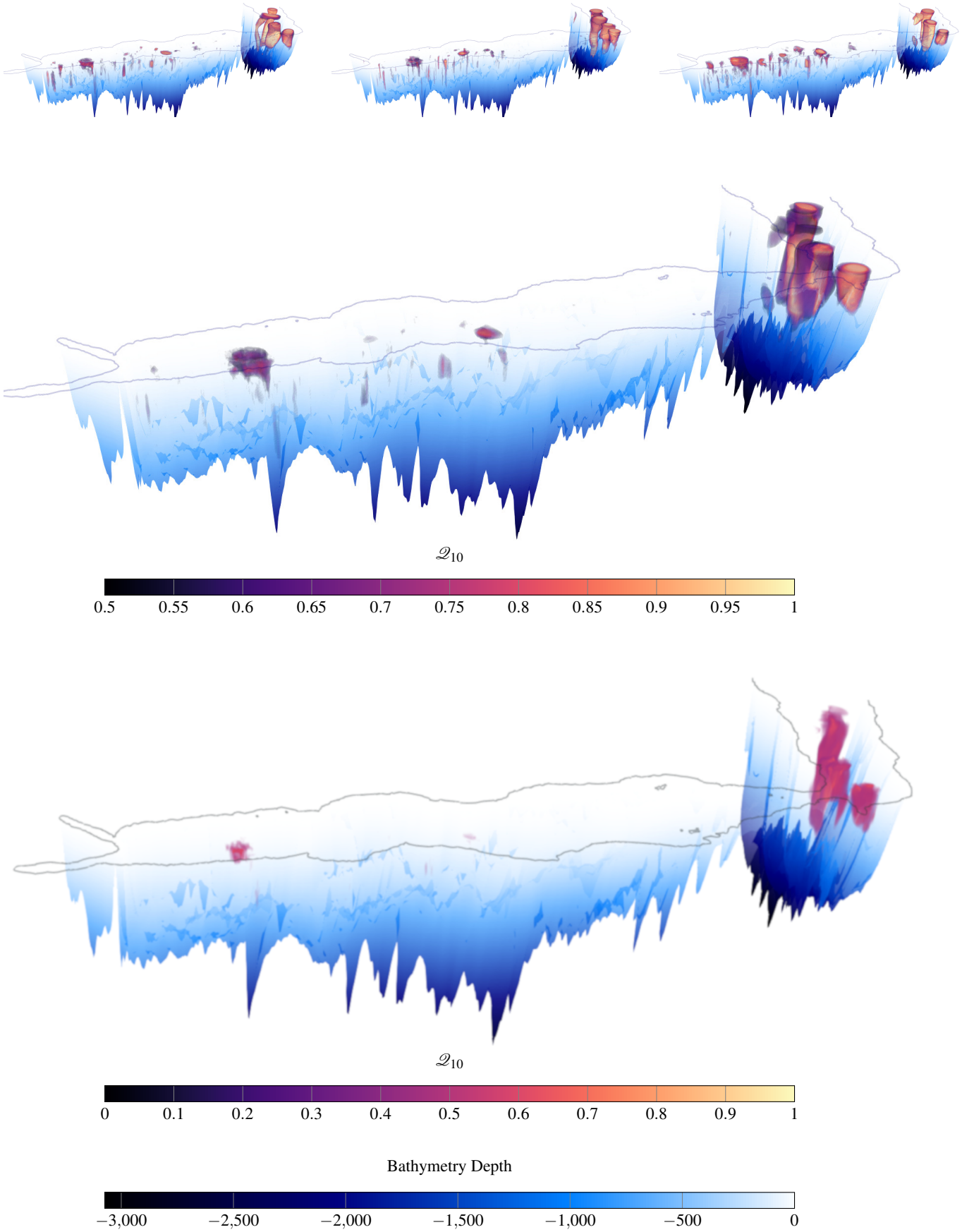

Figure 4: Top: $\mathscr{Q}_{10}$ of $\mathbf{v}_{\{1,2,3\}}$ at time $t = 200$h. Middle: Mean of $\mathscr{Q}_{10}$ for $\mathbf{v}_{\{1,2,3\}}$; Bottom Mean of $\mathscr{Q}_{10}$ for $\mathbf{v}_{\{1,2,3,4,5,6\}}$;

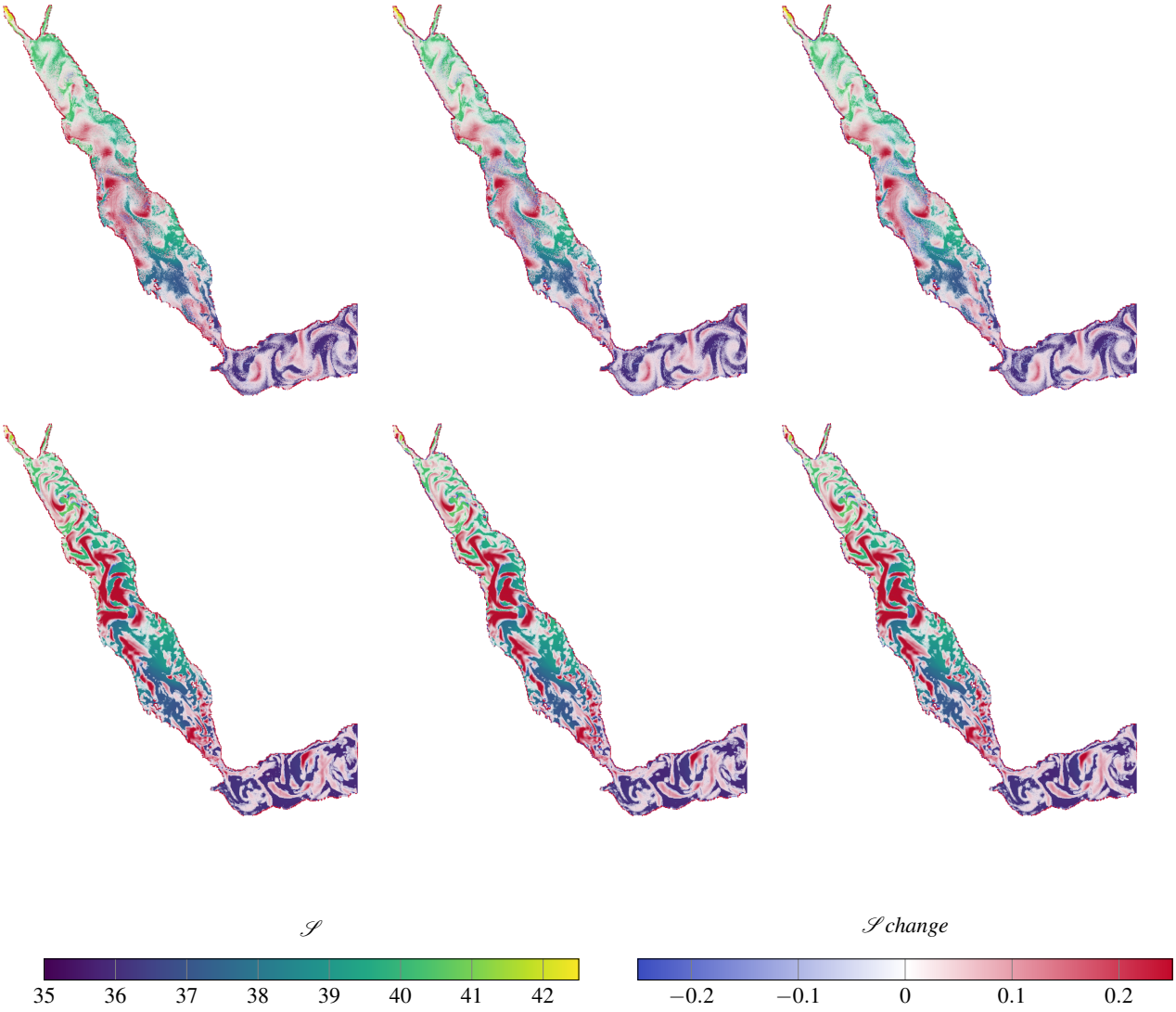

Figure 5: Top: three consecutive timesteps of $\mathbf{v}_1$. Bottom: three consecutive timesteps of $\mathbf{v}_{mean}$. Left : $t = 0$h. Mid: $t = 0$h 15m. Right: $t = 0$h 30m. Particles color code the $\mathscr{S}$ change per hour

Figure 6: Top: $\mathbf{v}_1$. Mid: $\mathbf{v}_2$. Bottom: $\mathbf{v}_3$. Left : $t = 0$h. Mid: $t = 100$h. Right: $t = 200$h.

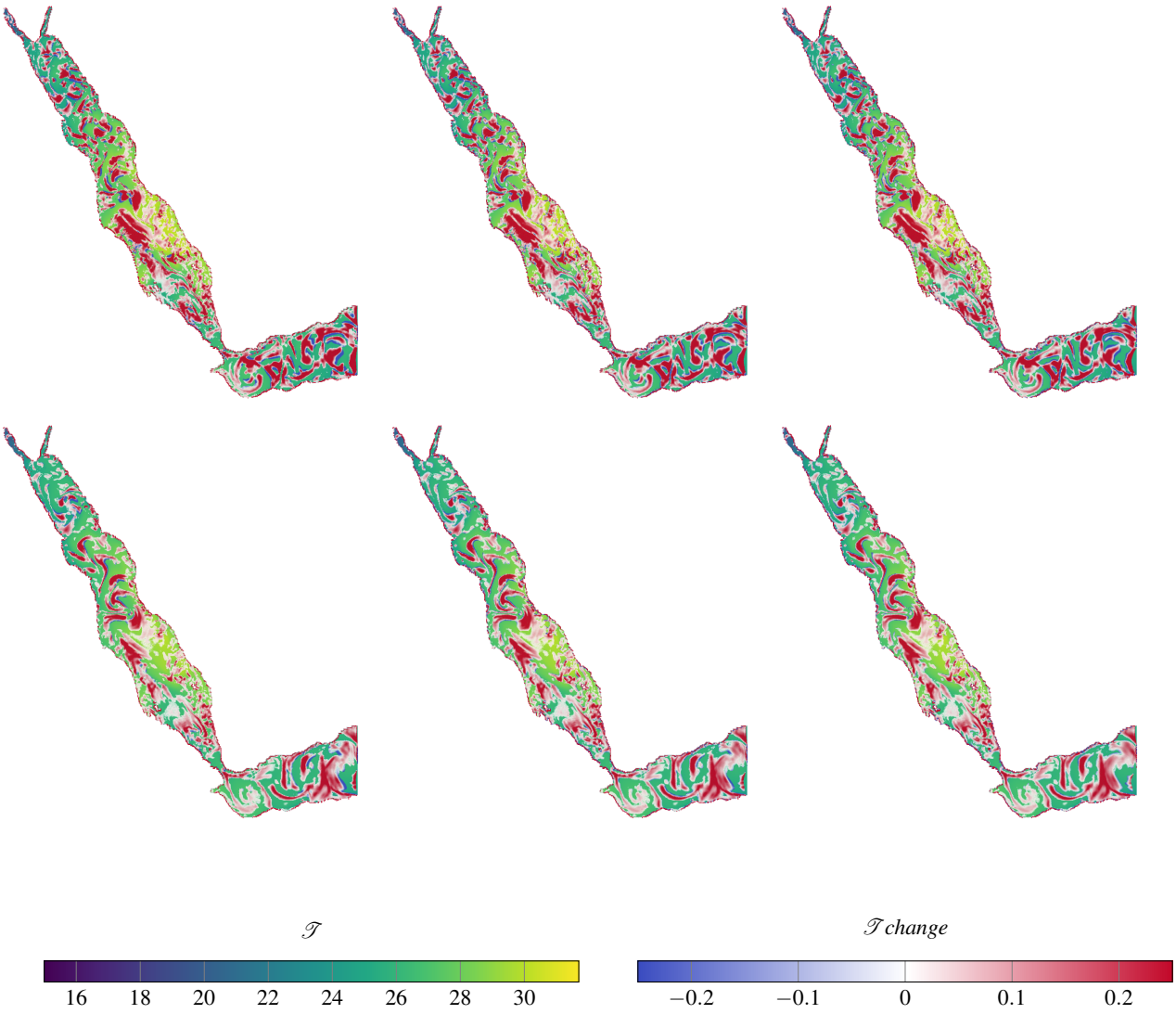

Figure 7: Top: three consecutive timesteps of $\mathbf{v}_1$. Bottom: three consecutive timesteps of $\mathbf{v}_{mean}$. Left : $t = 0$h. Mid: $t = 0$h 15m. Right: $t = 0$h 30m. Particles color code the $\mathscr{T}$ change per hour.

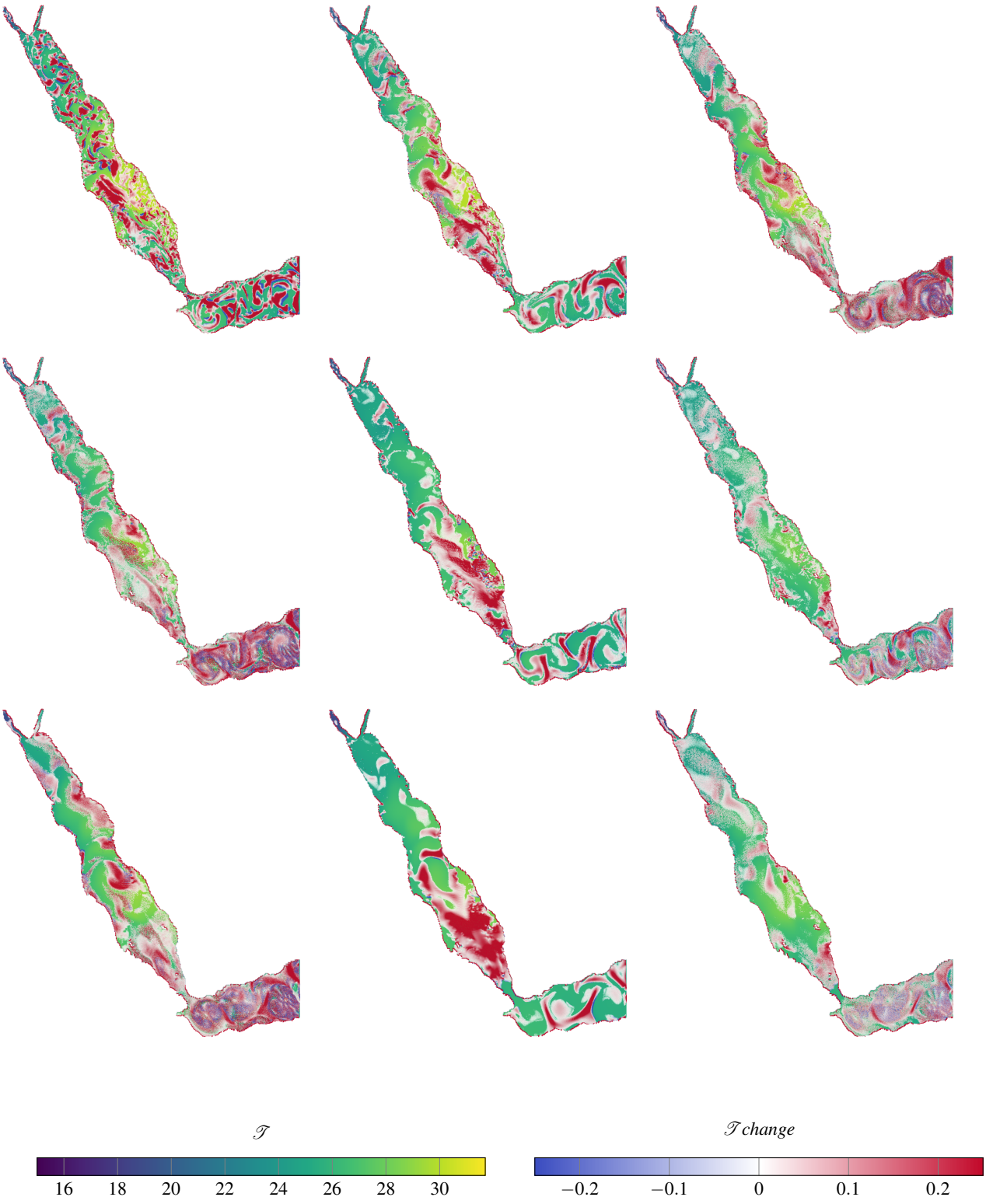

Figure 8: Top: $\mathbf{v}_1$. Mid: $\mathbf{v}_2$. Bottom: $\mathbf{v}_3$. Left : $t = 0$h. Mid: $t = 100$h. Right: $t = 200$h.